Organic & Biomolecular Chemistry

Accepted Manuscript

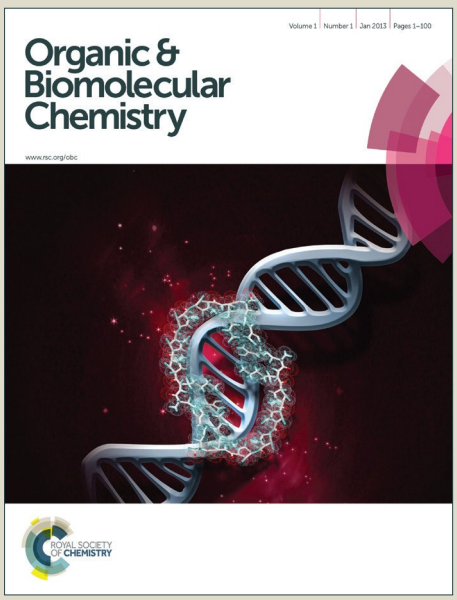

ROYAL SOCIETY OF CHEMISTRY

www.rsc.org/obc

Organic & Biomolecular Chemistry RSCPublishing

PAPER

IDB-containing low molecular weight short peptide as efficient DNA cleavage reagent

Cite this: DOI: 10.1039/x0xx00000x

Chunying Ma,[a] Huan Chen,[a] Chao Li,*[a] Jin Zhang[a] and Renzhong Qiao*[a,b]

Received 00th January 2012,
Accepted 00th January 2012

DOI: 10.1039/x0xx00000x

www.rsc.org/

Artificial nucleases have attracted significant interest due to their abilities in accelerating DNA cleavage, which makes the possibility of genome manipulation. However, compared with natural nucleases, currently available artificial nucleases have low cleavage efficiency, especially those metal-free artificial nucleases. Thus, it is still a challenge to develop highly efficient metal-free artificial nucleases via a non-oxidative pathway. We here designed and prepared a group of rigid bis-amine-grafted PASP conjugates (PASP-IDB), and investigated their abilities to induce DNA double-strand cleavage. The detailed assays showed that in the absence of metal ions, these short peptide conjugates can effectively break phosphodiester linkage at a relative low concentration and at physiological conditions through hydrolytic process, giving the 10^7-fold rate acceleration over uncatalyzed double-strand DNA. The probable mechanism verified by control experiments revealed that IDBs and free carboxyl groups in PASP synergically catalyzed DNA cleavage. Additionally, the effects of degrees of substitution on cleavage activity were studied, and results indicated the existence of minimum building blocks of PASP-IDB for efficient DNA cleavage. The results of our study have implications for the design of short peptide-based molecules as new artificial nucleases and may provide strategy for developing safe and efficient metal-free DNA cleavage reagents.

Introduction

DNA is exceptionally stable and difficult to be hydrolyzed under physiological conditions with a half-life hydrolysis rate of about 200 million years, which primarily due to the repulsion between the negatively charged backbone and potential nucleophiles.[1] However, the cleavage of DNA is of increasing importance in biotechnology, medicine and other fields, because this will offer many applications for manipulation of genes, design of structural probes and development of novel therapeutics.[2] As a result, artificial nucleases have attracted significant interest due to their accelerating DNA cleavage abilities. In this field, transition metal complex have been extensively studied in the last decade, but studies devoted to metal-free artificial nucleases are not frequent.[3] In fact, in the absence of metal ions, DNA cleavage is considered to be safer for the development of biotechnology and gene therapy, including the use of photo-induced processes[4] for treatment of cancer. Hence, a series of organic molecules such as guanidinium derivatives,[5] peptides[6] and polyamines[7] have been pushed forward to study their DNA cleavage abilities in the absence of metal ions, and also many efforts have been devoted to optimize their DNA cleavage activities.[8] In particular, Lu's group synthesized a metal-free artificial nuclease containing guanidinoethyl and hydroxyethyl side arms, and the DNA cleavage was achieved at a relative low concentration (0.1 mM), giving 10^7-fold rate acceleration over uncatalyzed double-strand DNA.[9] Yavin's group successfully designed a cyclic peptide scaffold which can promote DNA cleavage at physiological conditions and micromolar concentrations in the absence of metal ions.[10] Therefore, design and synthesis of metal-free molecules with efficient DNA cleavage abilities are highly desired.

Recently, we have reported a new family of poly(aspartic acid) (PASP) grafting cyclic polyamine conjugates (PASP-cyclen) which are able to effectively induce DNA cleavage in the absence of metal ions with a high-yield linearization product.[11] We surmised the probable mechanism that free carboxyl groups in the PASP skeleton often served as a nucleophile, while the polyamine can serve as a proton-donating or -accepting group to reduce electron density in phosphate, which was liable to breakage of the phosphodiester bond. Owing to the previous observations, we are intrigued by the idea that how about rigid structure molecules instead of cyclic polyamines conjugated to PASP skeleton act as DNA cleavage reagents. It is regarded that the introduction of rigid structures is of great significant because planar molecules could have ability to intercalate into nucleobases that were restricted

within narrow limits to reduce random of cleavage. Bis(2-benzimidazolyl-methyl)amine (IDB) as a rigid candidate was selected to be conjugated with the PASP skeleton, because over the last two decades many original and modified IDBs have attracted more attention as vital and ubiquitous structural units supporting artificial DNA cleavage and recognition agents, no matter what metal ions assist or not.[12]

In this work presented here, we therefore synthesized the title compound of IDB-grafted PASP conjugates (PASP-IDB, Scheme 1), and investigated the abilities of interaction with DNA, including intercalation and bond breakage by agarose gel electrophoresis, fluorescence quenching and circular dichroism (CD). A group of control compounds were also designed and evaluated to further explore a possible DNA cleavage mechanism and structure activity relationship of PASP-IDB conjugates, as shown in Scheme 1. In addition, different degrees of substitution (DS) of PASP-IDB were prepared to understand the capacity of nucleophilic attacking that depends on the amount of valid grafters.

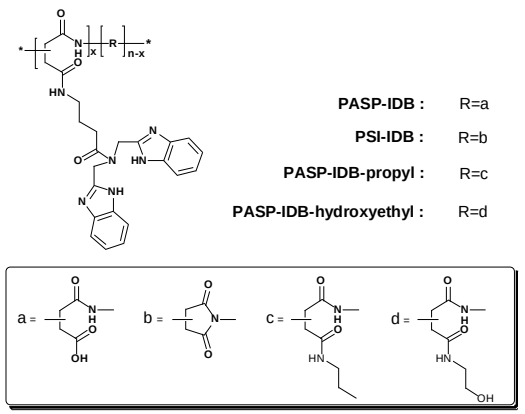

Scheme 1 Chemical structures of PASP-IDB and its control compounds PSI-IDB, PASP-IDB-propyl and PASP-IDB-hydroxyethyl.

Results and discussion

Cleavage of plasmid DNA

MALDI analysis of PASP-IDB gave number-average ($\bar{M}n$) and weight-average ($\bar{M}w$) molecular weights of 1281 and 1382 Da, respectively (see Experimental procedures section). The polydispersity (PD) value was calculated as 1.0 which didn't exceed 1.2, *i.e.* the practical PD limit in which MALDI can correctly reveal the molecular weight distribution.[13] And molar quantity of PASP-IDB is calculated by the ratio of mass to $\bar{M}n$. Thus, we can calculate the amounts of PASP-IDB in per unit mass concentration and further decide the molar concentration of PASP-IDB for DNA cleavage in agarose gel electrophoresis.

Initially, concentration-dependence assays of PASP-IDB were performed under physiological conditions (37 ℃, pH = 7.4), and the results are shown in Fig. 1(a). The supercoiled DNA (Form I) is converted to nicked DNA (Form II) with the increasing of concentration of PASP-IDB while the linear DNA (Form III) is detected. Up to 0.12 μM of PASP-IDB interacted with the plasmid, supercoiled DNA completely disappears in agarose gel electrophoresis and nicked/linear forms instead (Fig. 1(a), lane 9). As the control, no meaningful change was detected when 0.12 μM of free IDB was added into system under the same conditions (Fig. 1(b), Lane 9). And also, it is hard to monitor the presence of linear DNA over the tested concentration range. The observations above revealed that the catalytic activity was remarkably enhanced due to IDB grafted onto the PASP moiety. It should be noted that the appearance of linear DNA induced by a relative low concentration indicated that the conjugates not only remarkably promoted the ability to break double strands of DNA, but also reduced the random of cleavage.

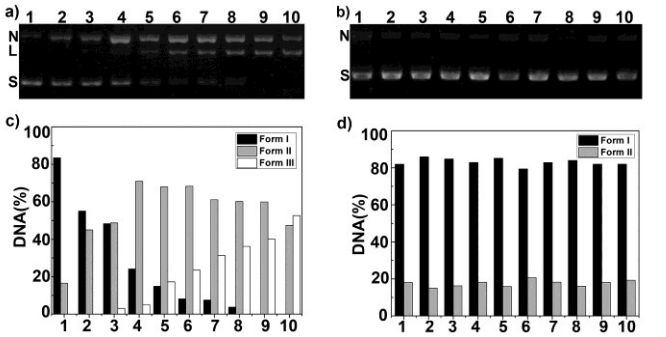

Fig. 1 Concentration dependence of plasmid pUC18 DNA (0.05 $\mu g \cdot \mu L^{-1}$) cleavage by (a) PASP-IDB (DS = 14.2%) and (b) IDB in 40 mM pH 7.4 Tris-HCl buffer at 37°C for 12 h. Lane 1: DNA control; Lanes 2-10: 1.6, 3.2, 7.9, 31.6, 63.2, 80.0, 110.6, 126.4 and 158.1 nM, respectively. Quantitation of % various DNA forms per lane by (c) PASP-IDB and (d) IDB. N: nicked DNA; L: linear DNA; S: supercoiled DNA.

Further evidence for the effect of PASP-IDB in the cleavage reaction is exhibited by time-dependence assays in Fig. 2(a). The kinetic plots indicate that the extent of supercoiled DNA cleavage varies exponentially with the reaction time, giving pseudo first-order kinetics with an apparent first-order rate constant (K_{obs}) of 0.186 ± 0.006 h^{-1} (Fig. 2(b)). The catalytic rates are about 10^7 times higher than that of DNA cleavage in the absence of catalyst (10^{-8} h^{-1}).[14] However, in the case of free IDB, no detectable change in nicked and linear forms as well as original plasmid is observed over the same time range (Fig. S6, SI). The results indicated that PASP-IDB can more efficiently promote the cleavage rate of plasmid DNA than that induced by free IDB under physiological conditions. To avoid any effect due to residual metal contamination involved in DNA cleavage induced by PASP-IDB, the control experiment using metal chelating agent EDTA (1 mM) was carried out. As shown in Fig. S7, no inhibition of DNA cleavage occurs in the presence of EDTA (Lane 5), which demonstrates that PASP-IDB can cleave DNA without the participation of any metal ions.

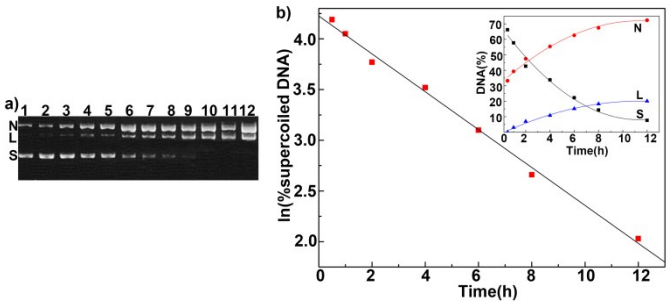

Fig. 2 Time dependence of plasmid pUC18 DNA (0.05 $\mu g \cdot \mu L^{-1}$) cleavage by (a) PASP-IDB (0.12 μM, DS = 14.2%) in 40 mM pH 7.4 Tris-HCl buffer at 37°C. Lane 1: control; Lanes 2-12: 0.5, 1, 2, 4, 6, 8, 12, 14, 16, 20 and 24 h, respectively. (b) Plot of ln(% supercoiled DNA) vs reaction time. Inset of Fig. 2(b) is the plot of DNA(%) vs reaction time. N: nicked DNA; L: linear DNA; S: supercoiled DNA.

In addition, we tried to get data of kinetic studies for nicked or linear DNA formation, and the plot by ln(% nicked or linear DNA) vs time was obtained. (Fig. S 10, SI) However, straight lines were not obtained in plots ln(% nicked or linear DNA) vs time, and the kinetic data, derived from gels similar to the K_{obs} depicted by Fig. 2, were not obtained. In Tonellato's work,[15] a straight line was obtained in plots of ln(% nicked DNA) vs reaction time, giving a K_{obs} of the formation of nicked DNA. Meanwhile, Tonellato reported that the decreasing nicked DNA was observed with increasing of reaction time, which suggests that the loss of nicked DNA may contribute to form linear one. In our current study, however, the nicked form is strictly increasing over the time range tested, which may indicate that ss- and ds cleavage are kinetically independent.

Subsequently, in order to assess whether the observed linearization induced by PASP-IDB represents a non-random linearization process, the statistical test of double-strand cleavage was applied.[16] Such analysis assumes a Poisson distribution of the strand cuts and calculates average number of single (n_1) and double (n_2) strand breaks from the fraction of supercoiled and linear DNA present after the reaction. The Freifelder-Trumbo relation suggests that approximately 120 ssb are required per dsb if the process is completely random.[17] Table 1 shows the statistical results of DNA linearization experiments of PASP-IDB performed under a variety of reaction conditions. However, at all times the range of n_1/n_2 values (5-22) is significantly smaller than expected from a completely random process, indicating that double-strand (ds) cleavage we observed is the true ds-cleavage instead of an accumulation of random single-strand (ss) breaks.

Table 1 DNA linearization (n1/n2) activities of PASP-IDB as function of reaction conditions.[a]

Entry	c/nm	T/h	Number of ss-breaks (n_1) and ds-breaks (n_2) per molecule		n_1/n_2
			n_1	n_2	
1	3.2	12	0.697	0.031	22
2	63.2	12	2.241	0.309	7
3	110.6	12	2.776	0.567	5
4	120.6	1	0.522	0.030	17
5	120.6	2	0.779	0.767	10
6	120.6	4	0.971	0.121	8
7	120.6	6	1.338	0.197	7

[a] pUC 18 DNA, 40 mM pH 7.4 Tris-HCl buffer 37 ℃.

To investigate the mechanism of DNA cleavage promoted by PASP-IDB, reactions in the presence of typical scavengers[18] for singlet oxygen (NaN_3), for hydroxyl radical (DMSO and *t*-BuOH) and for superoxide (KI) were carried out. As shown in Fig. 3(a), no significant inhibition effect on the DNA cleavage is observed in the presence of any scavengers, which rules out ROS involvement in the cleavage process. Therefore, DNA cleavage by PASP-IDB may occur via a hydrolytic path not an oxidative path. In addition, a hydrolytic mechanism was also supported by the T4 ligation experiment. As shown in Fig. 3(b), recovered linear DNA or smaller fragments were linked by treatment with T4 DNA ligase that provided sufficient evidence for DNA hydrolysis cleavage, because DNA linkage in the presence of T4 DNA ligase required the terminal groups of these fragments providing 3'-hydroxyls and 5'-phosphates. These results clearly suggested that PASP-IDB did hydrolyze DNA.

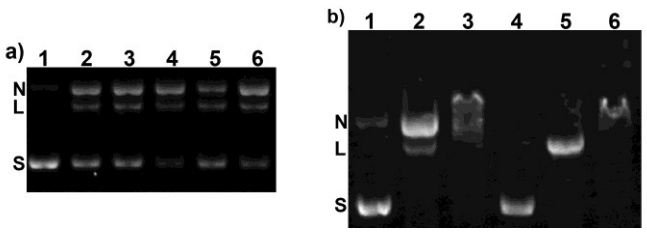

Fig. 3 (a) Inhibition studies on the cleavage of plasmid pUC18 DNA (0.05 $\mu g \cdot \mu L^{-1}$) by PASP-IDB (0.12 μM, DS = 14.2 %) in 40 mM pH 7.4 Tris-HCl buffer at 37°C for 12 h. Lane 1: DNA control; Lane 2: DNA with PASP-IDB; Lanes 3-6: DNA with PASP-IDB in the presence of NaN_3 (0.2 M), DMSO (0.2 M), *t*-BuOH (0.2 M) and KI (0.2 M), respectively. (b) Ligation of DNA cleavage fragments by T4 ligase. Lane 1: DNA control; Lane 2: recovered nicked DNA; Lane 3: recovered nicked DNA treated with T4 DNA ligase for 16 h at 16°C; Lane 4: DNA control; Lane 5: recovered linear DNA; Lane 6: recovered linear DNA treated with T4 DNA ligase for 16 h at 16°C. N: nicked DNA; L: linear DNA; S: supercoiled DNA.

Control assays for exploring the necessity of the "ungrafted" carboxyl groups

To further evaluate whether the "ungrafted" carboxyl groups of PASP-IDB are necessary in DNA cleavage process, a group of control compounds PSI-IDB, PASP-IDB-propyl and PASP-IDB-hydroxyethyl were designed and synthesized with the same degrees of IDB grafted (from the same intermediate PSI-IDB). As shown in Fig. 4, no detectable DNA cleavage appears in the presence of PSI-IDB without free carboxyl groups under

the same conditions, suggesting that the "ungrafted" active chain moieties of PASP-IDB may in favour of DNA cleavage. When the "ungrafted" carboxyl groups were replaced by chain propyl groups to generate PASP-IDB-propyl, it also does not cleave DNA under the same conditions. However, when the propyl groups were replaced by hydroxyethyl groups, DNA can be cleaved in spite of low efficiency. Thus, according to the comparison between the propyl analogue with the hydroxyethyl analogue. it can be concluded that catalytic action of -OH as potential nucleophilic group may be necessary in the "ungrafted" side chains of PASP skeleton in DNA cleavage process.

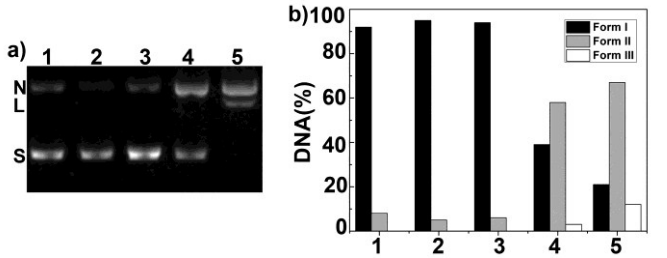

Fig. 4 (a) Comparison of DNA cleavage ability to plasmid pUC 18 DNA (0.05 $\mu g \cdot \mu L^{-1}$) among PSI-IDB, PASP-IDB-propyl, PASP-IDB-hydroxyethyl and PASP-IDB at the concentration of 0.12 μM in 40 mM pH 7.4 Tris-HCl buffer at 37°C for 12 h. Lane 1: DNA control; Lane 2: PSI-IDB; Lane 3: PASP-IDB-propyl; Lane 4: PASP-IDB-hydroxyethyl; Lane 5: PASP-IDB. (b) Quantitation of % various DNA forms per lane. N: nicked DNA; L: linear DNA; S: supercoiled DNA.

Fluorescence titration

The binding ability of compounds to DNA was reported to affect DNA cleavage in most cases and the three common binding modes including intercalation, grooving binding and electrostatic interaction, can be evaluated by fluorescence titration assays based on displacement of ethidium bromide.[6c] Here, fluorescence emission experiments were carried out to compare the DNA binding affinity of PASP-IDB (DS = 14.2%) and free IDB, and both fluorescence changes are recorded as shown in Fig. 5. When free IDB of 80 μM added to the EB-DNA system, the fluorescence intensity can reduce about 15%. However, the addition of PASP-IDB (DS = 14.2%) to EB-DNA system can substantially induce fluorescence intensity decrease by up to 51.2% with the same concentration of quenching agent. When the fluorescence intensity is plotted against concentration of quenching agent according to Stern-Volmer equation[19] (Fig. 5(c)), the quenching constant K given by the ratio of the slop to the intercept is 0.3 and 0.004 for PASP-IDB (DS = 14.2%) and free IDB, respectively, and the data indicate that PASP-IDB has higher binding affinity to DNA than free IDB at the same concentration. The interaction between IDB and DNA was apparently enhanced due to the introduction of PASP skeleton, which is accordance with the results in agarose gel electrophoresis. Meanwhile, the apparent binding constant (K_{app}) is calculated as 4.9×10^6 and 1.6×10^3 for PASP-IDB (DS = 14.2%) and free IDB, respectively. In spite of its high K_{app}, the title compound was supposed to interact with DNA by electrostatic interaction.[20] This is due to the introduction of PASP skeleton that may restrict IDB molecules within narrow space and lead to the accumulation of electrostatic interaction. The hypothesis is consistent with our previous report about PASP-cyclen.[11] In addition, an obvious hyperchromicity effect and blue shift in UV-Vis absorption spectra of PASP-IDB with increasing concentration of DNA (Fig. S11, SI) further demonstrate strong interactions between PASP-IDB and DNA, which may be attributed to the existence of electrostatic binding or to partial uncoiling the helix structure, exposing more bases of DNA.[21] Hence, it can be concluded that the introduction of PASP skeleton could result in more DNA binding affinity which has an influence on DNA cleavage ability, that is, the modification of PASP backbone promoted small molecular reagents to effectively bind with DNA and realize hydrolysis cleavage.

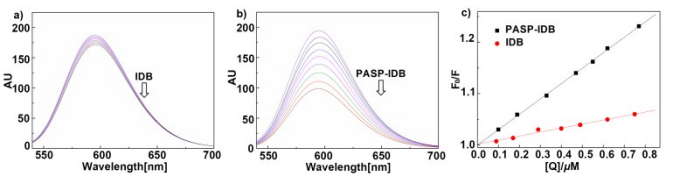

Fig. 5 Fluorescence quenching by (a) IDB/CT-DNA and (b) PASP-IDB (DS = 14.2%) /CT-DNA at pH 7.4 10 mM Tris-HCl buffer with 10 mM NaCl with quencher concentration of 0-80 μM (from top to bottom). (c) Plots of fluorescence quenching of CT-DNA by IDB (●) and PASP-IDB (■).

Circular Dichroism (CD)

Conformational changes of DNA interacting with molecules can be tested by CD experiments. Free B-type DNA shows a typical CD spectrum with a positive band near 275 nm due to base stacking and a negative band near 245 nm due to right-handed helicity.[22] It is generally accepted that classical intercalation enhances the intensities of both the bands stabilizing the right-handed B conformation of CT-DNA while simple groove binding and electrostatic interaction of small molecules show little or no perturbation on the base-stacking and helicity bands.[23] The addition of IDB to the DNA solution induces little CD signal change, indicating no remarkable intercalation between double-strand and IDB planar molecule (Fig. 6(a)). As shown in Fig. 6(b), the positive band of CT-DNA slightly decreases in intensity on addition of PASP-IDB, indicating that it might be a result of electrostatic interaction, while the negative band undergoes slight reductions almost without shift in the band positions, suggesting DNA remains in the B-type conformation with some helicity losses.[24] The absence of any detectable CD signals at 310-400 nm is the proof of the absence of minor groove binding between DNA and PASP-IDB. The observations showed that PASP-IDB as cleavage reagent does not change the configuration of DNA.

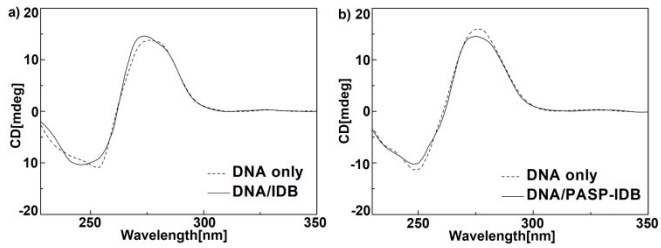

Fig. 6 CD spectra of (a) DNA only and DNA/IDB at N/P ratio 5/1 (dash line: DNA only; solid line: DNA/IDB complex) and (b) DNA only and DNA/PASP-IDB (DS = 14.2%) at N/P ratio 9/1 (dash line: DNA only; solid line: DNA/PASP-IDB complex).

Effect of degree of substitution on DNA cleavage

We next investigated the effect of different degrees of substitution (DS) of PASP-IDB on DNA cleavage, and results are shown in Table 1. When the concentration of PASP-IDB is 8.3×10^{-3} μM, the amounts of nicked DNA induced by PASP-IDB with the DS of 14.2%, 26.2%, and 33.3% are 72%, 83%, and 75%, respectively (Table 1, entries 4, 5 and 6). However, the cleavage only gives nicked products with the amounts of 39% and 43% in the presence of PASP-IDB with DS of 5.0% and 9.1%, respectively (Table 1, entries 2 and 3). These data showed that, generally speaking, the ability of PASP-IDB to induce DNA double-strand cleavage is gradually enhanced with the increasing of the amounts of IDB grafted. However, the most striking activity appeared when 26.2% IDB was grafted on PASP as cleavage molecules, inducing 14% of linear products. It means that about every three aspartic acid (Asp) monomer has grafted one IDB molecule, suggesting that the length and position of basic unit of PASP-IDB may be suitable to give the optimal combination towards DNA, and thus giving higher DNA cleavage ability. PASP-IDB with other DS may not have optimal structures due to the basic unit too long or too short, resulting in lower DNA cleavage abilities. Herein, minimum building blocks for PASP-IDB may exist, contributing to efficiently cleave DNA.

Table 2 Comparison of plasmid pUC18 DNA cleavage efficiency of PASP-IDB with different DS[a] (Fig. S9, SI)

Entry	DS (%)	DNA (%)		
		Form I	Form II	Form III
1	Control	68	32	-
2	5.0	61	39	-
3	9.1	57	43	-
4	14.2	25	72	3
5	26.2	3	83	14
6	33.3	21	75	4

[a] Cleavage reactions were carried out in 40 mM pH 7.4 Tris-HCl buffer 37 ℃ for 12 h.

Proposed process in a transphosphorylation pathway

Phosphodiester bonds of DNA have comparable stability in terms of half-life for spontaneous hydrolysis. When organic functional groups are exploited as catalytic groups for phosphodiester bonds hydrolysis, it is necessary to achieve collaboration among two or more catalytic groups. Catalytic action of carboxyl groups in a transphosphorylation and transaclytion reaction has been widely reported.[25] Carboxyl-based catalyst can act both as binding sites recognizing ammonium or guanidinium groups of the protein and as catalytic groups playing the catalytic roles similar to the Asp residues of aspartic proteases.[26] Additionally, two proximal imidazole groups are involved as key catalytic groups acting as general acid or nucleophile in the ribonuclease-catalyzed hydrolysis of phosphodiester bonds.[27] These results provide supporting evidence for the current proposed mechanism.

A possible process of DNA cleavage induced by PASP-IDB is speculated as shown in Scheme 2. In spite of the rigid structure, the distance between imidazole moieties and phosphate groups is close enough because of the electrostatic interactions, easily resulting in the form of hydrogen bonds between N-H and P-O. It is necessary for the following cleavage of phosphodiester, because polar interactions such as hydrogen-bonding and electrostatic interaction between the substrate and the enzyme contribute significantly to the stabilization of the transition states, and reduce effectively the charge density around the phosphate group. The electropositive phosphorus is liable to be attacked by surrounding nucleophilic groups. The ungrafted carboxyl in PASP skeleton as probable nucleophilic group may assist in achieving transphosphorylation reaction. This is consistent with our previous research.[11]

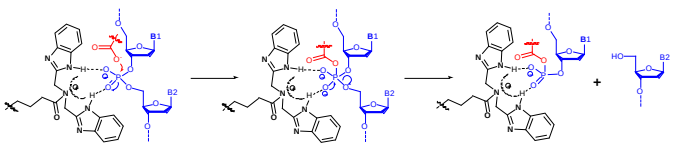

Scheme 2 Possible mechanism of DNA cleavage induced by PASP-IDB.

Conclusions

In this study, we tried to introduce a rigid bis-amine IDB to PASP skeleton to get a promising DNA cleavage reagent. The preliminary gel electrophoresis assays suggest that efficient DNA double-strand cleavage can be achieved at low concentration of PASP-IDB and at physiological conditions via a metal-free hydrolytic path. A probable mechanism is presumed that partly protonated IDB molecules could effectively reduce the charge density in around phosphate group, which provides a possibility that the "ungrafted" carboxyl groups as nucleophile cleave DNA. The degree of substitution of PASP-IDB has the influence on the ability of DNA cleavage, which demonstrates that every three Asp monomer grafted by one IDB molecule could be suitable structure to give the optimal combination towards DNA and exerted higher DNA cleavage ability than other degrees of substitution. These results are in excellent agreement with our previous reports. This observation, along with the structural similarity of both grafted molecules, provides a good strategy for developing effective metal-free artificial nucleases based on short peptide conjugates.

Experimental procedures

Materials and instrumentation

Details MS (ESI) mass spectral data were recorded on a Finnigan LCQDECA mass spectrometer. ^{1}H NMR and ^{13}C NMR spectra were measured on a Bruker AV600 spectrometer and chemical shifts in ppm are reported relative to internal Me_4Si ($CDCl_3$) or (CF_3COOD). All other chemicals and reagents were obtained commercially and used without further purification. Electrophoresis apparatus was using a Biomeans Stack II-Electrophoresis system, PPSV-010. Bands were visualized by UV light and photographed, recorded on an Olympus Grab-IT 2.0 Annotating Image Computer System. The molecular weight (MW) of the compounds was measured by Maldi-Tof (Bruker Autoflex). Electrophoresis grade agarose and plasmid DNA (pUC18) were purchased from Promega Corporation. Calf thymus DNA (CT-DNA) was purchased from Sigma (USA) Company and used as received.

Synthesis and characterization of PASP-IDB and its control compounds

The title compound of PASP-IDB and its control compounds are mainly prepared according to relative literature.[11] The route of synthesis and the NMR spectra are shown in SI Scheme S1 and Figs. S1-S4, respectively. The molecular weight (MW) range of PASP and PASP-IDB are given in SI Fig. S5. The degree of substituted IDB is calculated through ^{1}H NMR spectrum (see Supporting Information). The final product PASP-IDB was prepared in several batches with variable degrees of substituted IDB.

Maldi-Tof MS

Maldi-Tof MS was carried out on a Bruker Autoflex operating in reflected mode. 2-(4-Hydroxyphenylazo)-benzoic acid (HABA) was used as matrix, and NaCl or KCl was used as cationizing reagent. Samples were dissolved in H_2O at a concentration of 1.0 μg $\cdot$mL^{-1}. HABA was dissolved in dioxane at a concentration of 0.05 M. Sample (20 μL) and matrix (80 μL) solutions were mixed, and then 80 μL of 0.02 M NaCl or KCl was added. Finally, 1 μL of the resulting mixture was placed on the Maldi plate.

Polymeric compounds are generally defined by average molecular weight (*i.e.*, number-average molecular weight ($\bar{M}n$) and weight-average molecular weight ($\bar{M}w$) and polydispersity (PD):[28]

$$\bar{M}n = \Sigma M_i n_i / \Sigma n_i \quad (1)$$

$$\bar{M}w = \Sigma (M_i n_i) M_i / \Sigma M_i n_i \quad (2)$$

$$\mathrm{PD} = \bar{M}w / \bar{M}n \quad (3)$$

Where M_i and n_i is the molecular weight and the abundance of the ion i, respectively. The average molecular weight information was calculated in a Microsoft Excel worksheet using the data extracted form MALDI spectra.

Gel electrophoresis experiments

Electrophoresis experiments were performed with plasmid DNA (pUC18). In a typical experiment, supercoiled pUC18 DNA (5 μL, 0.05 μg μL^{-1}) in Tris-HCl buffer (40 mM, pH = 7.4) was treated with different concentration catalyst, followed by dilution with the Tris-HCl buffer to a total volume of 80 μL. The samples were then incubated at different temperature and time intervals, and quenched with loading buffer containing 0.5 M EDTA, and loaded on a 1% agarose gel containing 1.0 μg $\cdot$mL^{-1} ethidium bromide (EB). Electrophoresis apparatus consisted of a Biomeans Stack II Electrophoresis system, PPSV-010. Electrophoresis was carried out at 85 V for 1 h in TAE buffer, and bands were visualized by UV light and photographed, recorded on an Olympus Grab-IT 2.0 Annotating Image Computer System.

Analysis of DNA linearization.

Double-stranded DNA cleavage chemistry was studied further by quantification of forms III and II. The formation of single-strand breaks (ssb) and double-strand breaks (dsb) was quantified by gel electrophoresis on plasmid DNA, and the average numbers of ssb's (n_1) and dsb's (n_2) per molecule were quantitated using a standard model, which assumes a Poisson distribution of cleavage sites.[16]

The fraction of linear DNA after scission chemistry, f(III), is related to the number (n_2) of double-stranded breaks per molecule given by the first term of a Poisson distribution (eq 1).[16]

$$f(\mathrm{III}) = n_2 \exp(-n_2) \quad (1)$$

The sum of single-stranded (n_1) and double-stranded (n_2) breaks per molecule ($n_1 + n_2$) was determined from the fraction f(I) of supercoiled DNA remaining after treatment with the PASP-IDB conjugates.[16]

$$f(\mathrm{I}) = \exp[-(n_1 + n_2)] \quad (2)$$

The Freifelder-Trumbo relation (eq 2) shows that the number of double-strand breaks expected from coincidences of random single-stranded breaks is less than 0.01 per molecule, that is, $n_1/n_2 > 120$.[16a] Consequently, from comparison of the ratio of n_1 and n_2 (n_1/n_2) relative to 120, one can determine if the linearization of DNA resulted from random or nonrandom cleavage. In these studies, both n_1 and n_2 were calculated using eqs 1 and 2. The Friefelder-Trumbo relationship was further developed by Cowan and co-workers.[29] We analysed our results by both the Friefelder-Trumbo and Cowan methodologies.

Fluorescence Quenching Assay

Fluorescence spectra were recorded on a Hitachi model F-4500 spectrofluorimeter, with excitation and emission band bass: 10 nm (λ_{ex} = 520 nm, λ_{em} = 620 nm). 10 mg $\cdot$mL^{-1} solution of IDB

and PASP-IDB were titrated into the DNA-EB solution at pH 7.4 10 mM Tris-HCl buffer with 10 mM NaCl.

Apparent binding constants (K_{app}) of the ligands with CT-DNA were estimated and compared by measuring the loss of EtBr fluorescence as a function of added ligand. The K_{app} values were calculated from: K_{EtBr} [EtBr] = K_{app} [ligand],[30] where [EtBr] and K_{EtBr} are the concentration and binding constant of EtBr, respectively, and [ligand] is the concentration of ligand at 50% of maximal EtBr fluorescence. The binding constant of EtBr was taken to be 1×10^7 ([EB] = 3.9 μM).[31]

The relative binding propensity of the two compounds to CT-DNA was determined by fitting the emission intensity to the classical Stern-Volmer equation $I_0/I = 1 + Kr$, where I_0 and I are the fluorescence intenseties in the absence and the presence of the quencher, K is the linear Stern-Volmer quenching constant dependent on the ratio of r_{bE} (the ratio of [EB] bound to [DNA]), and r is the ratio of $[quencher]_{total}$ to [DNA].[32] Fig. 5 shows the plot of I_0/I versus [quencher]/[DNA], and the quenching constant K is given by the ratio of the slope to the intercept.

CD experiments

Circular dichroism (CD) experiments were performed under a continuous flow of nitrogen using a the Jasco-810 spectropolarimeter. A path length cell of 1 cm was used, and all experiments were performed at room temperature. The sample was titrated into the 60 μg·mL^{-1} DNA solutions (at pH 7.4 10 mM Tris-HCl buffer with 10 mM NaCl) with a final concentration of 80 μM. The standard scan parameters for all experiments used a wavelength range from 400 to 220 nm. Sensitivity was set at 100 mdeg and scan speed of 200 nm per minute. Three scans were made and the average value of them was calculated.

Acknowledgements

Support of this research by the National Nature Science Foundation of China (Nos. 21372024, 21202005 and 21232005) is gratefully acknowledged.

Notes and references

a State Key Laboratory of Chemical Resource Engineering, Beijing University of Chemical Technology, Beijing, 100029, P. R. China
b State Key Laboratory of Medicinal Chemical Biology, Nankai University, Tianjin, 300071, P. R. China
† Electronic Supplementary Information (ESI) available: [Spetra for all new compounds, degrees of substitution of PASP-IDB, and gel electrophoresis experiments]. See DOI: 10.1039/b000000x/

1 (a) C. S. Jeung; J. B. Song; Y. H. Kim and J. Suh, *Bioorg. Med. Chem. Lett.*, 2001, **11**, 3061; (b) F. H. Westheimer, *Science*, 1987, **235**, 1173.

2 (a) C. Metcalfe and J. A. Thomas, *Chem. Soc. Rev.*, 2003, **32**, 215; (b) C. Liu, M. Wang, T. Zhang and H. Sun, *Coord. Chem. Rev.*, 2004, **248**, 147; (c) J. R. Morrow and O. Iranzo, *Curr. Opin. Chem. Biol.*, 2004, **8**, 192.

3 (a) K. A. Schug and W. Lindner, *Chem. Rev.*, 2005, **105**, 67; (b) A. M. Piatek, M. Gray and E. V. Anslyn, *J. Am. Chem. Soc.*, 2004, **126**, 9878; (c) S. H. Wan, F. Liang, X. Q. Xiong, L. Yang, X. J. Wu, P. Wang, X. Zhou and C. T. Wu, *Bioorg. Med. Chem. Lett.*, 2006, **16**, 2804.

4 B. Breiner, K. Kaya, S. Roy, W. Y. Yang and I. V. Alabugin, *Org. Biomol. Chem.*, 2012, **10**, 3974.

5 (a) U. Scheffer, A. Strick, V. Ludwig, S. Peter, E. Kalden and M. W. Göbel, *J. Am. Chem. Soc.*, 2005, **127**, 2211; (b) C. Gnaccarini, S. Peter, U. Scheffer, S. Vonhoff, S. Klussmann and M. W. Göbel, *J. Am. Chem. Soc.*, 2006, **128**, 8063.

6 (a) C. T. Cheng, V. Lo, J. Chen, W. C. Chen, C. Y. Lin, H. C. Lin, C. H. Yang and L. Sheh, *Bioorg. Med. Chem.*, 2001, **9**, 1493; (b) Y. Feng, S. Cao, A. Xiao, W. Xie, Y. Li and Y. Zhao, *Peptides*, 2006, **27**, 1554; (c) Z. F. Li, H. L. Chen, L. J. Zhang and Z. L. Lu, *Bioorg. Med. Chem. Lett.*, 2012, **22**, 2303; (d) M. Sun, Y. Ma, S. Ji, H. Liu and Y. Zhao, *Bioorg. Med. Chem. Lett.*, 2004, **14**, 3711.

7 (a) M. Q. Wang, J. L. Liu, J. Y. Wang, D. W. Zhang, J. Zhang, F. Streckenbach, Z. Tang, H. H. Lin, Y. Liu, Y. F. Zhao and X. Q. Yu, *Chem. Commun.*, 2011, **47**, 11059; (b) J. Li, J. Zhang, Q. S. Lu, Y. Yue, Y. Huang, D. W. Zhang and H. H. Lin, *Eur. J. Med. Chem.*, 2009, **44**, 5090.

8 (a) W. Y. Yang, B. Breiner, S. V. Kovalenko, C. Ben, M. Singh, S. N. Legrand, Q. X. A. Sang, G. F. Strouse, J. A. Copland and I. V. Alabugin, *J. Am. Chem. Soc.*, 2009, **131**, 11458. (b) S. V. Kovalenko and I. V. Alabugin, *Chem. Commun.*, 2005, 1444.

9 X. Sheng, X. M. Lu, J. J. Zhang, Y. T. Chen, G. Y. Lu, Y. Shao, F. Liu and Q. Xu, *J. Org. Chem.*, 2007, **72**, 1799.

10 S. Alkhader, A. Ezra, J. Kasparkova, V. Brabec and E. Yavin, *Bioconjugate Chem.*, 2010, **21**, 1425.

11 C. Li, F. F. Zhao, N. Y. Huang, X. Y. Liu, Y. Liu, R. Z. Qiao and Y. F. Zhao, *Bioconjugate Chem.*, 2012, **23**, 1982.

12 (a) R. J. Sundberg and R. B. Martin, *Chem. Rev.*, 1974, **74**, 471; (b) E. Reisner, V. B. Arion, A. Eichinger, N. Kandler, G. Giester, A. J. L. Pombeiro and B. K. Keppler, *Inorg. Chem.*, 2005, **44**, 6704; (c) F. A. Tanious, D. Hamelberg, C. Bailly, A. Czarny, D. W. Boykin and W. D. Wilson, *J. Am. Chem. Soc.*, 2004, **126**, 143; (d) Y. Miao, M. P. H. Lee, G. N. Parkinson, A. B. Parra, M. A. Ismail, S. Neidle, D. W. Boykin and W. D. Wilson, *Biochemistry*, 2005, **44**, 14701; (e) D. Renneberg and P. B. Dervan, *J. Am. Chem. Soc.*, 2003, **125**, 5707; (f) R. L. Lombardy, F. A. Tanious, K. Ramachandran and R. R. Tidwell, *J. Med. Chem.*, 1996, **39**, 1452.

13 (a) G. Montaudo, D. Garozzo, M. S. Montaudo, C. Puglisi and F. Samperi, *Macromolecules*, 1995, **28**, 7983; (b) Y. Suzuki, Y. Esumi, H. Koshino and Y. Doi, *Macromol. Biosci.*, 2005, **5**, 853.

14 (a) D. S. Sigman, A. Mazumder and D. M. Perrin, *Chem. Rev.*, 1993, **93**, 2295; (b) N. H. Williams, B. Takasaki, M. Wall and J. Chin, *Acc. Chem. Res.*, 1999, **32**, 485.

15 C. Sissi, F. Mancin, M. Gatos, M. Palumbo, P. Tecilla and U. Tonellato, *Inorg. Chem.*, 2005, **44**, 2310.

16 (a) B. T. David Freifelder, *Biopolymers*, 1969, **7**, 681; (b) L. F. Povirk, W. Wübker, W. Köhnlein and F. Hutchinson, *Nucleic Acids Res.*, 1977, **4**, 3573.

17 Y. Jin, M. A. Lewis, N. H. Gokhale, E. C. Long, J. A. Cowan, *J. Am. Chem. Soc.*, 2007, **129**, 8353.

18 Y. Zhao, J. Zhu, W. He, Z. Yang, Y. Zhu, Y. Li, J. Zhang and Z. Guo,

Chem. Eur. J., 2006, **12**, 6621.
19 Y. Cao and X. W. He, *Spectrochim. Acta, Part A*, 1998, **54**, 883.
20 Q. H. Zhou and P. Yang, *Acta Chim. Sinica*, 2005, **63**, 71.
21 (a) W. Tang, H. Xu, E. J. Park, M. A. Philbert, R. Kopelman, *Biochem. Biophys. Res. Commun.*, 2008, **369**, 579; (b) R. F. Pasternack, E. J. Cibbs, J. J. Villafranca, *Biochemistry*, 1983, **22**, 2406; (c) C. Pratviel, J. Bernadou, B. Meunier, *Adv. Inorg. Chem.*, 1998, **45**, 51.
22 (a) P. Lincoln, E. Tuite and B. Nordén, *J. Am. Chem. Soc.*, 1997, **119**, 1454; (b) B. Nordén and F. Tjerneld, *Biopolymers*, 1982, **21**, 1713; (c) S. Mahadevan and M. Palaniandavar, *Inorg. Chem.*, 1998, **37**, 3927.
23 (a) Y. X. Yin, J. H. Wen, Z. R. Geng, Y. Z. Li and Z. L. Wang, *Appl. Organometal. Chem.*, 2012, **26**, 671; (b) P. U. Maheswari and M. Palandavar, *J. Inorg. Biochem.*, 2004, **98**, 219.
24 (a) K. Karidi, A. Garoufis, N. Hadjiliadis and J. Reedijk, *Dalton. Trans.*, 2005, **4**, 728; (b) E. Gallori, C. Vettori, E. Alessio, F. G. Vilchez, R. Vilaplana, P. Orioli, A. Casini and L. Messori, *Arch. Biochem. Biophys.*, 2000, **376**, 156; (c) Y. Shao, X. Sheng, Y. Li, Z. L. Jia, J. J. Zhang, F. Liu and G. Y. Lu, *Bioconjugate Chem.*, 2008, **19**, 1840; (d) B. Ranjbar and P. Gill, *Chem. Biol. Drug. Des.*, 2009, **74**, 101.
25 J. Suh, *Acc. Chem. Res.*, 2003, **36**, 562.
26 H. Kim, Y. S. Chung, H. Paik, M. Kim and J. Suh, *Bioorg. Med. Chem. Lett.*, 2002, **12**, 2663.
27 (a) C. A. Deakyne and L. C. Allen, *J. Am. Chem. Soc.*, 1979, **101**, 3951; (b) M. P. Fitzsimons and J. K. Barton, *J. Am. Chem. Soc.*, 1997, **119**, 3379.
28 (a) T. W. D. Chan, P. K. Chan and K. Y. Tang, *Anal. Chim. Acta*, 2006, **556**, 226; (b) H. C. M. Byrd and C. N. McEwen, *Anal. Chem.*, 2000, **72**, 4568.
29 R. Cowan, C. M. Collis and G. W. Grigg, *J. Theor. Biol.*, 1987, **127**, 229.
30 S. Dhar, M. Nethaji and A. R. Chakravarty, *Inorg. Chem.*, 2005, **44**, 8876.
31 (a) S. Yellappa, J. Seetharamappa, L. M. Rogers, R. Chitta, R. P. Singhal and F. D'Souza, *Bioconjugate Chem.*, 2006, **17**, 1418; (b) R. C. Holmberg and H. H. Throp, *Anal. Chem.*, 2003, **75**, 1851; (c) D. L. Ma, C. M. Chen, F. M. Siu and K. Y. Yong, *Inorg. Chem.*, 2007, **46**, 740; (d) J. Kuwahare and Y. Sugiura, *Proc. Natl. Acad. Sci. U. S. A.*, 1998, **85**, 2459; (e) H. A. Benesi and J. H. Hildebrand, *J. Am. Chem. Soc.*, 1949, **71**, 2730.
32 (a) J. R. Lakowicz and G. Weber, *Biochemistry*, 1973, **12**, 4161; (b) M. Lee, A. L. Rhodes, M. D. Wyatt, S. Forrow and J. A. Hartley, *Biochemistry*, 1993, **32**, 4237; (c) L. J. Childs, J. Malina, B. E. Rolfsnes, M. Pascu, M. J. Prieto, M. J. Broome, P. M. Rodger, M. E. V. Sletten, A. Rodger and M. J. Hannon, *Chem. Eur. J.*, 2006, **12**, 4919; (d) J. Liu, T. Zhang, T. Lu, L. Qu, H. Zhou, Q. Zhang and L. Ji, *J. Inorg. Biochem.*, 2002, **91**, 269.

